sustainability

MDPI

Technical Note

Variation Characteristics of Hydrodynamic Coefficients of Two-Dimensional Rectangular Moonpool Resonance under Sway Motion

Zhouhao Zhang [1], Hongsheng Zhang [1], Yuxin Wang [1] and Yu Zhang [2,*]

[1] College of Ocean Science and Engineering, Shanghai Maritime University, Shanghai 201306, China
[2] College of Harbour, Coastal and Offshore Engineering, Hohai University, Nanjing 210024, China
* Correspondence: jessicazhang@hhu.edu.cn

Abstract: The phenomenon of sudden changes in hydrodynamic coefficients cannot be neglected when the resonance of a two-dimensional rectangular moonpool occurs; however, it may not be meaningful to discuss the detailed values of hydrodynamic coefficients when the resonance occurs. The analytical solution of the hydrodynamic coefficients of a two-dimensional rectangular moonpool under sway motion derived based on the linear potential flow theory is first improved. The improved analytical results and the results with the far-field method are then compared and verified. The results show that the hydrodynamic coefficients of a two-dimensional rectangular moonpool under sway motion change suddenly at the second resonant frequency, which was not found in the original analytical solution of damping coefficient.

Keywords: moonpool; resonance; hydrodynamic coefficient; analytical solution

Citation: Zhang, Z.; Zhang, H.; Wang, Y.; Zhang, Y. Variation Characteristics of Hydrodynamic Coefficients of Two-Dimensional Rectangular Moonpool Resonance under Sway Motion. *Sustainability* **2022**, *14*, 15952. https://doi.org/10.3390/su142315952

Academic Editors: Yuquan Zhang, Jianhua Zhang, Ling Zhou and Bin Huang

Received: 13 October 2022
Accepted: 25 November 2022
Published: 30 November 2022

1. Introduction

Most engineering ships and offshore platforms are equipped with a moonpool structure with openings at the bottom, and the water in the moonpool is connected to the outside. The fluid movement in the moonpool can be divided into vertical piston mode and horizontal sloshing mode [1]. On one hand, the moonpool can provide a stable marine operating environment for the drilling equipment and riser, and can improve the efficiency of wave energy conversion devices. On the other hand, when the external excitation frequency is the same as the natural frequency of the moonpool, fluid resonance occurs in the moonpool, which significantly affects the motion of the ship and the stability of navigation. Therefore, it is of great significance to study the resonant phenomenon of the fluid inside the moonpool as well as its hydrodynamic characteristics of the moonpool.

The natural modes of oscillation of the inner free surfaces of the moonpool are determined under the assumption of infinite water depth via the linearized potential flow theory, and the problem is addressed in two and three dimensions by Molin (2001) [2]. A numerical method for the study of sloshing in tanks with a two-dimensional flow was presented by Faltinsen (1978) [3]. The hydrodynamic interactions of water wave diffraction on a super large floating structure composed of numerous box-shaped modules were studied; a new resonant phenomenon, which is related to the draft of the structure, was revealed, and the relationship between the draft of the structure and the gap width and resonance frequencies was discussed by Miao et al. (2000) [4]. Combined theoretical and experimental studies of the two-dimensional piston-like steady-state motions of the fluid in a moonpool are presented, and a high-precision, analytically oriented, linear-potential-flow method was developed by Faltinsen et al. (2007) [5]. The equations for solving the radiation and diffraction problems of a two-dimensional rectangular moonpool were established via the linearized potential flow theory, the expressions of the hydrodynamic coefficients were derived, and the effect of the opening on the excitation force and hydrodynamic

coefficients was evaluated, by Zhou et al. (2013) [6]. Based on Zhou et al. (2013) [6], the radiation and diffraction problems of a two-dimensional rectangular moonpool in front of a straight wall at a finite water depth were studied by Zhang and Zhou (2013) [7]. Based on the CFD theory, a method that includes both numerical simulation and analysis of the ship added mass and damping coefficient was outlined for ships oscillating in waves by Zhu et al. (2009) [8]. Potential and N.-S. equation-based flows were numerically simulated around a two-dimension floating rectangular body with a moonpool using Fluent software, and the influences of the vorticity on the vertical motion of the moonpool under a forced heave motion were evaluated by Heo et al. (2014) [9]. The differences in the moonpool resonant frequencies between the fixed and free-floating conditions were studied using the radiation-diffraction code WAMIT, and the effect of the vessel configuration on the offset of the moonpool resonant frequencies was examined by Huang et al. (2019) [10]. Theoretical models for calculating the natural frequencies and modal shapes of two-dimensional asymmetric and symmetric moonpools in finite water depth were proposed by Zhang et al. (2019) [11]. In the case of a symmetric moonpool, single-mode approximations (SMA) have been derived and can be used to quickly estimate the natural frequencies of the piston and sloshing modes.

In this study, the analytical solution of a two-dimensional rectangular moonpool under the sway motion deduced in Zhou et al. (2013) [6] was improved, and the variation characteristics of the hydrodynamic coefficients at the second resonance frequency were supplemented. The far-field method results of the hydrodynamic coefficients were compared with the improved analytical results.

2. Analysis of the Original Analytical Solution

Suppose that a rectangular moonpool floats on the free surface of water, and the structure oscillates with a small amplitude under external excitation. The Cartesian coordinate system $Oxyz$ is obtained, where the Oxy plane coincides with the still water level, and the origin of the coordinate axis is located at the intersection of the symmetry axis of the moonpool and still water level. The water depth is h. Assuming that the rectangular moonpool is infinite in the y direction, the influence in the length direction can then be neglected. The moonpool and flow field can thus be simplified into a two-dimensional form, as shown in Figure 1, where the width of the moonpool is $2b$, the width of the opening is $2a$, the draft depth of the moonpool is h_1, and the height of the moonpool is h_2.

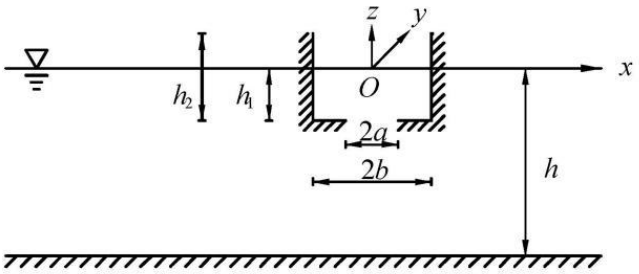

Figure 1. Sketch of two-dimensional flow field and rectangular moonpool.

The hydrodynamic force on a body can be obtained from the integration of the pressure based on the linear Bernoulli equation over the wetted body surface. For wave radiation due to body oscillation, Zhou et al. (2013) [6] provided the expression of the excitation force, τ_{pq}, in mode p due to the motion of unit amplitude in mode q:

$$\tau_{pq} = i\omega\rho \int_{S_b} \left[-i\omega\phi^{(q)}(x,z) \right] n_p dS = \rho\omega^2 \int_{S_b} \phi^{(q)} n_p dS \quad (1)$$

where, ω is the circular frequency, ρ is the water density, S_b represents the wetted body surface, $\phi^{(q)}$ is the normalized velocity potential of motion in mode q, and n_p is the normal direction of the wetted body surface.

The force due to wave radiation can be written in terms of the added mass μ_{pq} and damping coefficient λ_{pq}. The non-dimensional added mass μ_{pq} and damping coefficient λ_{pq} derived by Zhou et al. (2013) [6] are expressed as follows:

$$\mu_{pq} = Re(\tau_{pq}) / \left[2\rho h_1 \omega^2 b b^{(\delta_{3p}+\delta_{3q})}\right] \tag{2}$$

$$\frac{\lambda_{pq}}{\omega} = Im(\tau_{pq}) / \left[2\rho h_1 \omega^2 b b^{(\delta_{3p}+\delta_{3q})}\right] \tag{3}$$

where Re indicates that the real part of the complex function is taken, Im indicates that the imaginary part of the complex function is taken, and δ_{pq} is the Kronecker delta function given by

$$\delta_{pq} = \begin{cases} 0 & p \neq q \\ 1 & p = q \end{cases}. \tag{4}$$

After the authors' rederivation, it is inferred that the analytical solution derived by Zhou et al. (2013) [6] is accurate. However, we found that the numerical variation of the hydrodynamic coefficients, especially the damping coefficient under the sway motion at the second resonant frequency, cannot be accurately captured because the calculation accuracy is insufficient.

Assume $h = 3.0$ m, $h_1 = 1.0$ m, $2b = 1.0$ m, and $a/b = 0.8$. For this case, $2kb$ is the same as the value of k. The hydrodynamic coefficients of the moonpool were calculated according to the code provided by Dr. Zhou. It can be observed from Figure 2a that, under the heave motion, significant numerical changes in the added mass appear in the frequency range of $2kb = 0 \sim 1$, and two extrema, one large and one small, appear in this range. It can be observed from Figure 2b that, under the heave motion, significant numerical changes in the damping coefficient also appear in the same frequency range, and the extremum variation of λ_{22} corresponds to the value change of the added mass.

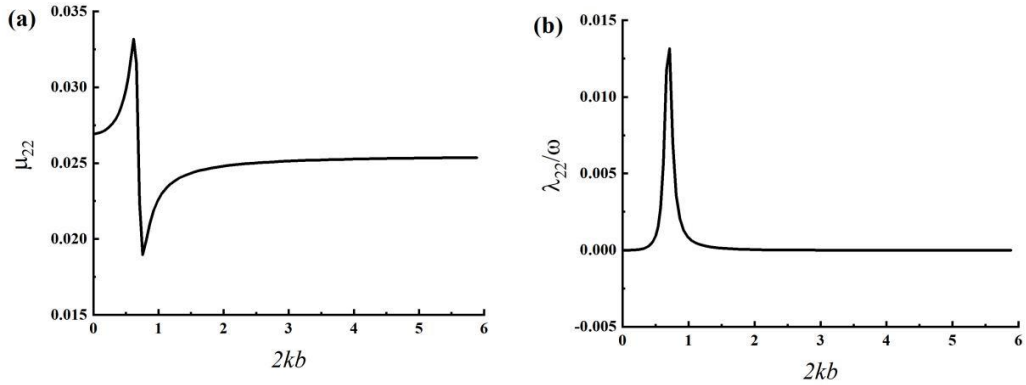

Figure 2. Analytical results of hydrodynamic coefficients of the moonpool under heave motion (by Zhou's program): (**a**) added mass; (**b**) damping coefficient.

It can be observed from Figure 3a that, under the sway motion, the first maximum of the added mass appears in the range of frequency $2kb = 0 \sim 1$. The positive and negative extrema of the added mass appear near the second resonant frequency of $2kb = 3.1$. It can be observed from Figure 3b that, under the sway motion, the peak of the damping coefficient also appears in the range of frequency $2kb = 0 \sim 1$, whereas the damping coefficient only fluctuates weakly near the second resonant frequency of $2kb = 3.1$, where the extremum of the added mass appears.

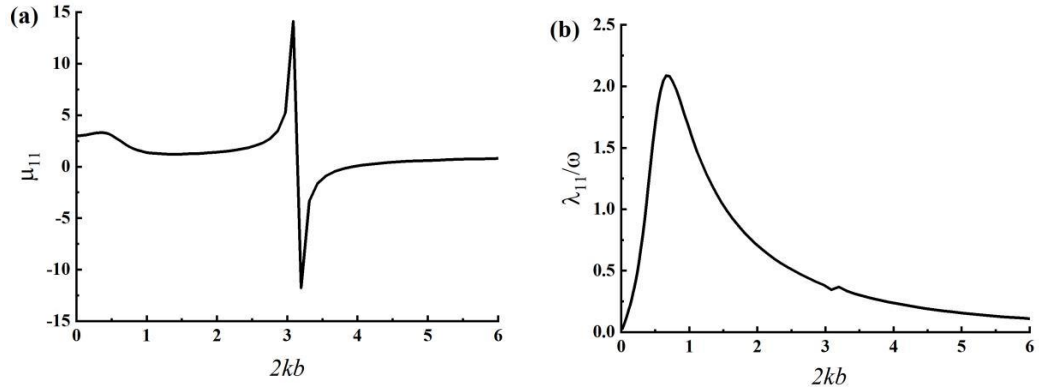

Figure 3. Analytical results of hydrodynamic coefficients of the moonpool under sway motion (by Zhou's program): (**a**) added mass; (**b**) damping coefficient.

In the code provided by Dr. Zhou, ω is given first, $\Delta\omega$ is taken as 0.1, and the wave number k is then obtained through iteration of the dispersion equation. The dispersion equation is expressed as follows:

$$\omega^2 = gk \tanh(kh) \tag{5}$$

where g is the gravitational acceleration. Furthermore, according to Equations (20)–(24) by Zhou et al. (2013) [6], the eigenvalues, α_n, β_n, and γ_n correspond to three different water depths, h, h_1, and h_2, respectively, and the subsequent solving is then carried out. Table 1 shows the calculated frequency, wave number, and increments of the wave number according to the method of Zhou. It can be observed from Table 1 that, with an increase in ω, the step size Δk gradually increases. Additionally, from a numerical point of view, Δk was greater than $\Delta\omega$. Although the given ω has an equal difference increment, k obtained by iteration does not change uniformly in an equal difference, and Δk is greater than $\Delta\omega$. This may lead to an inaccurate capture of the resonant frequency and thus, the variation in the damping coefficient near the resonant frequency is not captured.

Table 1. k and Δk under different ω.

ω	k	Δk
...	...	...
5.2	2.75637	0.10449
5.3	2.86340	0.10703
5.4	2.97248	0.10908
5.5	3.08359	0.11111
5.6	3.19674	0.11315
5.7	3.31193	0.11519
5.8	3.42915	0.11722
5.9	3.54842	0.11927
6.0	3.66972	0.12130
6.1	3.79307	0.12335
6.2	3.91845	0.12538

3. Solution Improvement and Comparative Analysis

3.1. Improvement of Analytical Solution

We adjust part of the analytical solution code of the hydrodynamic coefficients under sway motion, which is related to the solution of the wave number. The relevant parameters are the same as those described in Section 2. The program is changed to specify k first, then obtain ω using Equation (5), and then α_n, β_n and γ_n. The step size Δk was set to 0.1, and the comparisons between the adjusted new analytical results and original analytical results are shown in Figure 4. It can be observed from Figure 4a that, after the adjustment, the

value of the positive extremum of the added mass increases significantly near the second resonant frequency of $2kb = 3.1$ compared with the original one. As shown in Figure 4b, however, the damping coefficients are almost the same.

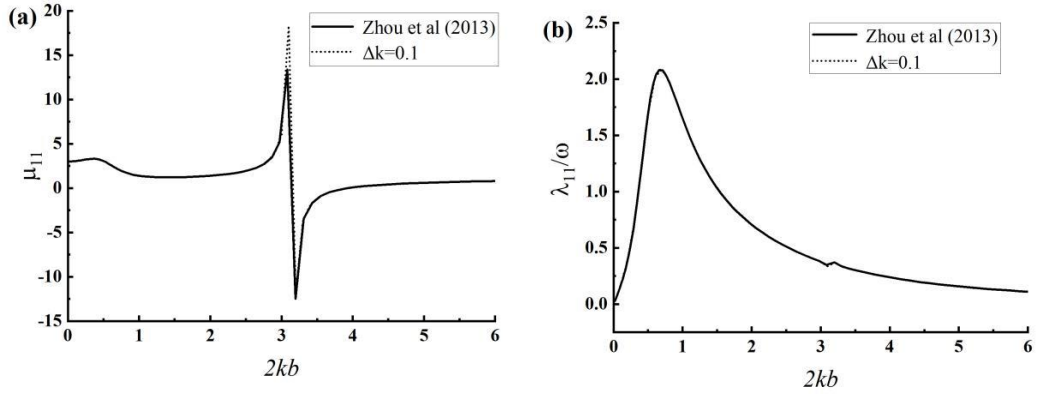

Figure 4. Comparison between the original analytical and improved results ($\Delta k = 0.1$) [6]: (**a**) added mass; (**b**) damping coefficient.

The Δk near the second resonant frequency ($2kb = 3.14$~3.15) is more carefully adjusted, and Δk is set as 0.01, 0.001, and 0.0001, respectively. The hydrodynamic coefficients for the different Δk values are shown in Figure 5. As shown in Figure 5a, when $\Delta k = 0.01$, the values of the two extrema of the added mass, which are 380.040 and -89.876 at $2kb = 3.14$ and 3.15, respectively, vary greatly compared with Δk=0.1. It can be observed from Figure 5b that, when $\Delta k = 0.01$, the damping coefficients, which are 0.00265 and 0.530 at $2kb = 3.14$ and 3.15, respectively, no longer fluctuate weakly near the second resonant frequency; instead, it shows an obvious numerical change. As shown in Figure 5c, when $\Delta k = 0.001$, the two extrema of the added mass, especially the negative extreme values, tend to infinity, which are 787.393 and $-10{,}580.496$ at $2kb = 3.141$ and 3.142, respectively. It can be observed from Figure 5d that, when $\Delta k = 0.001$, the minimum of the damping coefficient at $2kb = 3.140$ is 0.00265, and the maximum tends to infinity and appears at $2kb = 3.142$ with a value of 251.760. As shown in Figure 5e, when $\Delta k = 0.0001$, the two extrema of the added mass, which are 23,681.718 and $-10{,}580.496$ at $2kb = 3.1419$ and 3.1420, respectively, tend to infinity. As shown in Figure 5f, when $\Delta k = 0.0001$, the damping coefficient has a minimum of 0.00014 at $2kb = 3.1402$ and a maximum of 1129.184 at $2kb = 3.1419$. Regardless of the value of Δk, the damping coefficient is always greater than 0, which is in line with the physical reality. As mentioned above, if Δk is more accurate, then the second resonant frequency is captured more accurately. The damping coefficient also appears as an extremum near the second resonant frequency, and the value approaches infinity.

To observe the variation of the hydrodynamic coefficients more carefully with an accuracy of Δk, the hydrodynamic coefficients for different values of Δk are amplified in local details. Figure 6 shows the comparisons among the details of the added mass and damping coefficient near the second resonant frequency for different sizes of Δk. As shown in Figure 6, when $\Delta k = 0.0001$, near the second resonant frequency, the curves of the added mass and damping coefficient change more smoothly, and the resonant frequency is captured more accurately.

Figure 7 shows the comparisons among the details of the added mass and damping coefficient in finite numerical intervals for different sizes of Δk. It can be observed from Figure 7 that, regardless of Δk, the results of the added mass and damping coefficient are almost identical in finite numerical intervals.

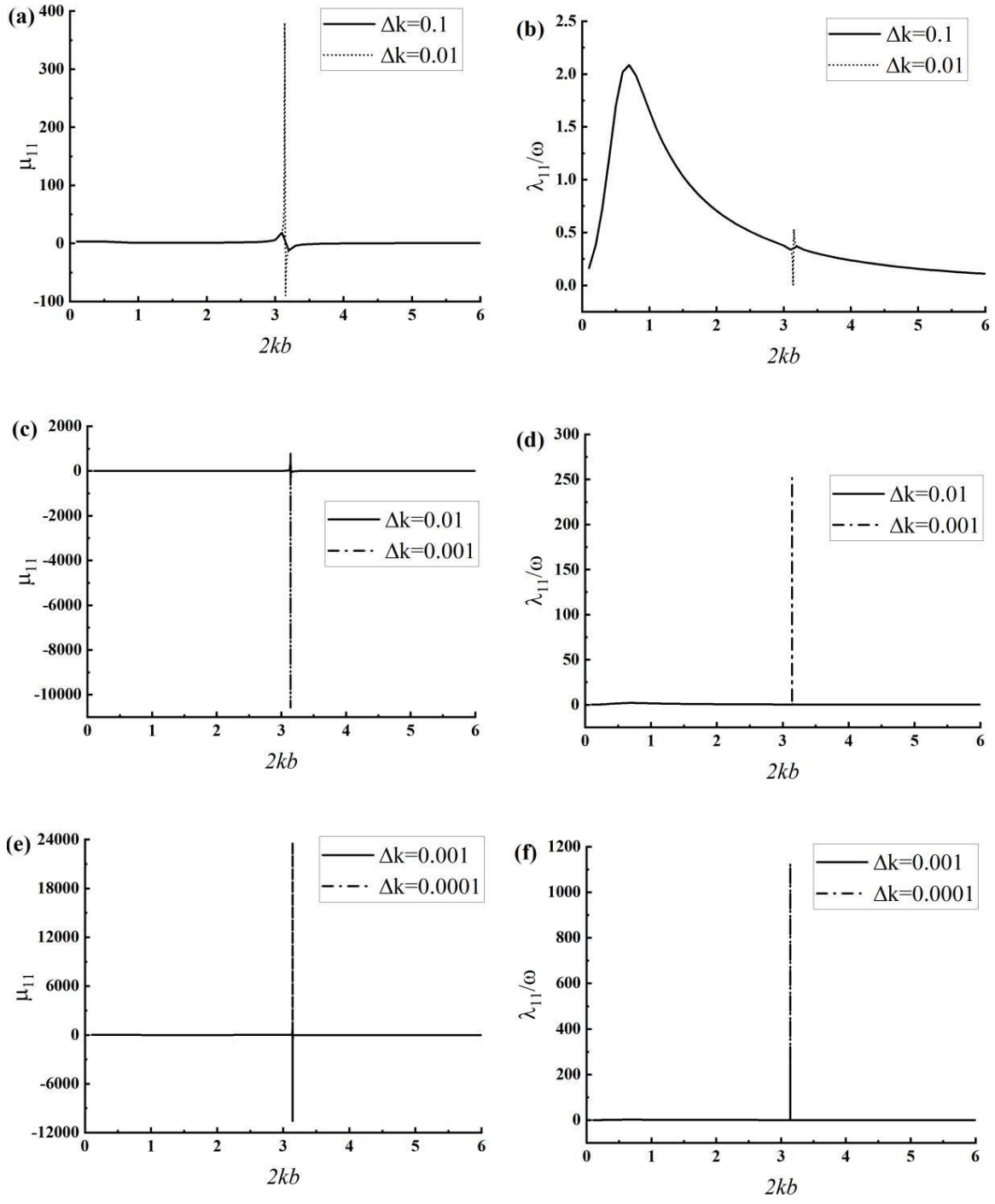

Figure 5. Comparisons of hydrodynamic coefficients with different increments of Δk: (**a**) added mass ($\Delta k = 0.1$, $\Delta k = 0.01$); (**b**) damping coefficient ($\Delta k = 0.1$, $\Delta k = 0.01$); (**c**) added mass ($\Delta k = 0.01$, $\Delta k = 0.001$); (**d**) damping coefficient ($\Delta k = 0.01$, $\Delta k = 0.001$); (**e**) added mass ($\Delta k = 0.001$, $\Delta k = 0.0001$); (**f**) damping coefficient ($\Delta k = 0.001$, $\Delta k = 0.0001$).

The analytical solutions discussed in this paper are based on the assumptions of an ideal fluid and a small motion amplitude. After the improvement of the solution process, from the above analyses and comparisons among the hydrodynamic coefficient results, it can be deduced that, although the values of the extrema of the two hydrodynamic coefficients at the second resonant frequency are different, their tendency to infinity is obvious.

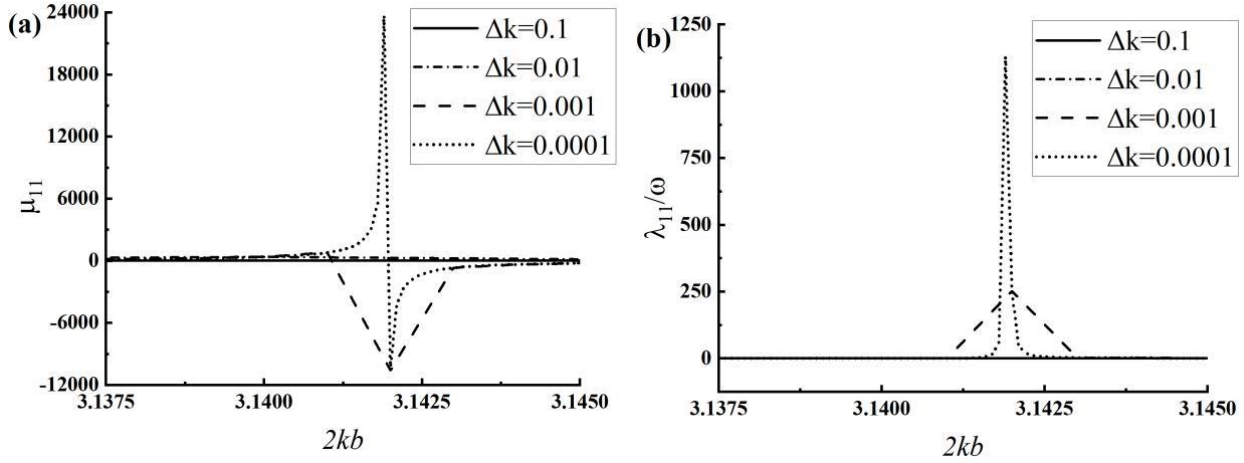

Figure 6. Comparisons of details of hydrodynamic coefficients near the second resonant frequency with different increments of Δ*k*: (**a**) added mass; (**b**) damping coefficient.

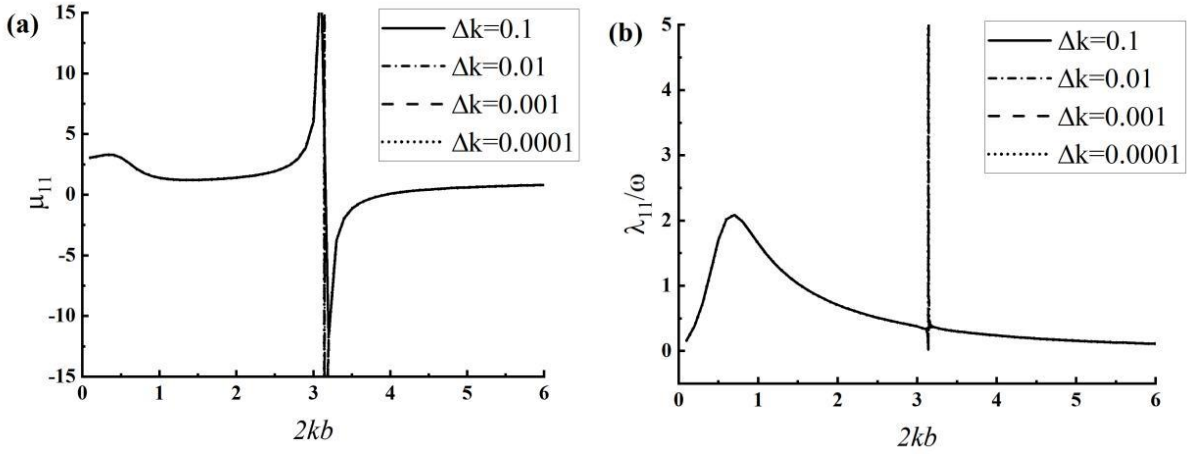

Figure 7. Comparisons of details of hydrodynamic coefficients in finite numerical intervals with different increments of Δ*k*: (**a**) added mass; (**b**) damping coefficient.

The point of resonance in the analytical solution discussed in this study is a singularity. The point of resonance was profound; however, it is regarded as an infinitesimal "point" in geometry, it does not exist, and all physical laws fail at that point. Therefore, the specific values of the hydrodynamic coefficients at the resonance point are meaningless. Moreover, infinity does not correspond to the physical reality; thus, it is not necessary to examine the specific values of the hydrodynamic coefficients in depth studies. However, the sudden change in hydrodynamic coefficients near the second resonant frequency is very important and cannot be neglected.

3.2. Comparison to Far-Field Results

The analytical solution discussed above is based on the near-field method, that is, the fluid force is calculated by integrating the pressure on the moonpool along the wetted body surface. The damping coefficient can also be calculated based on the wave amplitudes at infinity, which is referred to as the far-field method. The damping coefficient of a two-dimensional rectangular moonpool with the far-field method derived by Zhou et al. (2013) [6] is expressed as

$$\frac{\lambda_{pq}}{\omega} = \frac{gC_g\left(A_q^- A_q^{-*} + A_q^+ A_q^{+*}\right)}{2h_1 b^{1+\delta_{3p}+\delta_{3q}}\omega^3} \tag{6}$$

where

$$C_g = \frac{g}{2\omega}\tanh kh\left(1 + \frac{2kh}{\sinh 2kh}\right) \tag{7}$$

is the group velocity, A_q^+ and A_q^- are complex wave amplitudes at $x \to +\infty$ and $x \to -\infty$, respectively, and the superscript $*$ indicates a complex conjugate.

Figure 8 shows the comparisons between the damping coefficients of the moonpool under sway motion obtained using the two methods. This indicates that the results obtained with the two methods are in good agreement, which further proves that the improved analytical results are reasonable and correct.

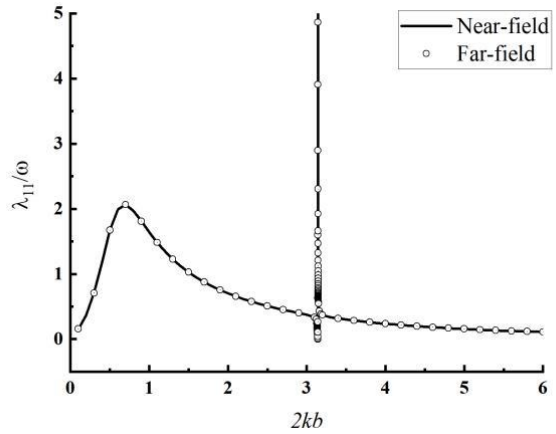

Figure 8. Comparison of damping coefficients with the near- and far-field methods.

3.3. Comparisons of Results with Different Openings

The hydrodynamic coefficients of the moonpool under sway motion with different a/b values are calculated to verify whether the improved analytical solution is applicable to the moonpool with different opening ratios. Assuming a/b as 0.2, 0.4, 0.6, and 0.8, respectively, the other parameters are the same as those in previous section. Figure 9 shows the comparisons among the hydrodynamic coefficients of the moonpool with different a/b values in finite numerical intervals. It can be observed that, under sway motion, the opening has little effect on the hydrodynamic coefficients, and the hydrodynamic coefficients have slight differences only at the first peak. For different a/b values, both the added mass and damping coefficients tend to be infinite near the second resonant frequency. Therefore, it is not accidental that the value of the damping coefficient tends to infinity at the resonant frequency; instead, it is universal.

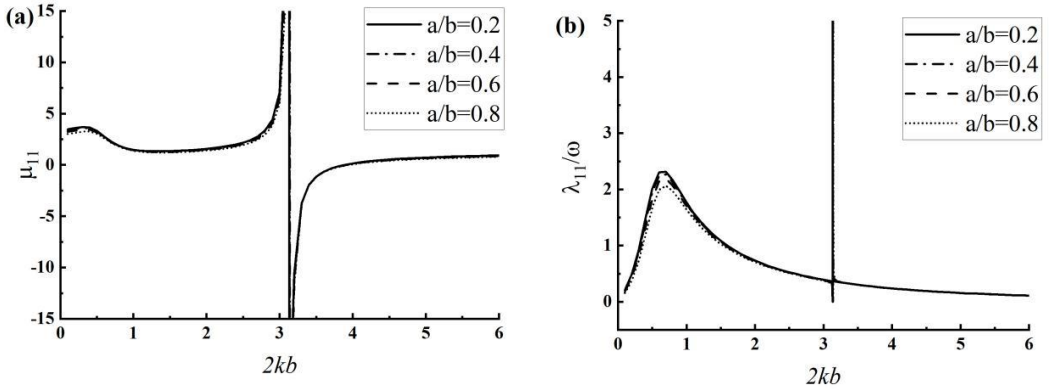

Figure 9. Comparison of hydrodynamic coefficients with different values of a/b: (**a**) added mass; (**b**) damping coefficient.

4. Conclusions

It is of great physical significance to discuss sudden changes in the hydrodynamic coefficients at the resonant frequency when a two-dimensional rectangular moonpool oscillates. In this study, the analytical solution of the hydrodynamic coefficients of a two-dimensional rectangular moonpool under sway motion based on the linear potential flow theory is improved. In the improved analytical solution, the phenomenon that the damping coefficient also appears as an extremum near the second resonant frequency was found. The variation characteristics of the hydrodynamic coefficients at the second resonant frequency of the moonpool, namely, the phenomenon in which the values of the added mass and damping coefficient tend to infinity at the second resonant frequency, is studied in detail. The improved analytical solution is verified by comparing the results of the near- and far-field methods and comparing the results under different opening ratios. In addition, we also simulated the forced oscillation motion of the moonpool using Fluent software, and the numerical results of the hydrodynamic coefficients are compared with the improved analytical solutions. Although there is no need to list the relevant calculation results, and the calculation method is also a commonly used method, the accuracy of the improved analytical solutions can be further illustrated from the perspective of numerical solutions. All the results show that the added mass and damping coefficient have extrema corresponding to each other at the resonant frequencies when the moonpool is under sway motion. The phenomenon in which the extremum appears cannot be neglected, although the detailed values of the extrema are insignificant for discussion.

Author Contributions: Conceptualization and methodology, Y.Z. and H.Z.; validation and formal analysis, Y.W., Z.Z. and H.Z.; writing—original draft preparation, Y.W., Z.Z. and H.Z.; writing—review and editing, Z.Z. and Yu Zhang; funding acquisition, Y.Z. and H.Z.. All authors have read and agreed to the published version of the manuscript.

Funding: This research was funded by National Natural Science Foundation of China (NSFC) (Grant Nos. 52201321 and 51679132). This work was also supported by Shanghai Frontiers Science Center of "Full Penetration" Far-Reaching Offshore Ocean Energy and Power.

Institutional Review Board Statement: Not applicable.

Informed Consent Statement: Not applicable.

Data Availability Statement: Not applicable.

Acknowledgments: This paper was completed after a thorough discussion with Wu G. X. His serious attitude toward scientific research was impressive. We express our sincere gratitude to Wu for taking time out of his busy schedule to answer the authors' questions.

Conflicts of Interest: The authors declare no conflict of interest.

References

1. Fukuda, K. Behavior of Water in Vertical Well with Bottom Opening of Ship, and its Effects on Ship-Motion. *J. Soc. Nav. Archit. Jpn.* **1977**, *1977*, 107–122. [CrossRef]
2. Molin, B. On the piston and sloshing modes in moonpools. *J. Fluid Mech.* **2001**, *430*, 27–50. [CrossRef]
3. Faltinsen, O.M. A Numerical Nonlinear Method of Sloshing in Tanks with Two-Dimensional Flow. *J. Ship Res.* **1978**, *22*, 193–202. [CrossRef]
4. Miao, G.P.; Ishida, H.; Saitoh, T. Influence of gaps between multiple floating bodies on wave forces. *China Ocean. Eng.* **2000**, *4*, 407–422.
5. Faltinsen, O.M.; Rognebakke, O.F.; Timokha, A.N. Two-dimensional resonant piston-like sloshing in a moonpool. *J. Fluid Mech.* **2007**, *575*, 359–397. [CrossRef]
6. Zhou, H.W.; Wu, G.X.; Zhang, H.S. Wave radiation and diffraction by a two-dimensional floating rectangular body with an opening in its bottom. *J. Eng. Math.* **2013**, *83*, 1–22. [CrossRef]
7. Zhang, H.-S.; Zhou, H.-W. Wave radiation and diffraction by a two-dimensional floating body with an opening near a side wall. *China Ocean. Eng.* **2013**, *27*, 437–450. [CrossRef]
8. Zhu, R.C.; Guo, H.Q.; Miao, G.P. A computational method for evaluation of added mass and damping of ship based on CFD theory. *J. Shanghai Jiaotong Univ. (Chin.)* **2009**, *43*, 198–203.

9. Heo, J.-K.; Park, J.-C.; Koo, W.-C.; Kim, M.-H. Influences of Vorticity to Vertical Motion of Two-Dimensional Moonpool under Forced Heave Motion. *Math. Probl. Eng.* **2014**, *2014*, 424927. [CrossRef]
10. Huang, H.Y.; Xu, X.; Zhang, X.S. Study on three-dimensional moonpool resonance of fixed and free-floating vessels. *Chin. J. Hydrodyn. (Chin.)* **2019**, *34*, 482–488.
11. Zhang, X.; Huang, H.; Song, X. On natural frequencies and modal shapes in two-dimensional asymmetric and symmetric moonpools in finite water depth. *Appl. Ocean. Res.* **2019**, *82*, 117–129. [CrossRef]